AIAA-87-0306
**The Role of Recirculation in Improving
Internal Mixing and Stability of Flames**

J. F. Driscoll, R. H. Chen and
V. Tangirala, Univ. of Michigan,
Ann Arbor, MI

AIAA 25th Aerospace Sciences Meeting
January 12-15, 1987/Reno, Nevada

THE ROLE OF RECIRCULATION IN IMPROVING
INTERNAL MIXING AND STABILITY OF FLAMES

J. F. Driscoll[*], R. H. Chen[**], V. Tangirala[†]
Department of Aerospace Enginering
University of Michigan
Ann Arbor, Michigan 48109-2140

Abstract

One goal of the present research program is to quantify and explain the observed increase in the fuel-air mixing rate in a flame that occurs when the internal recirculation is increased. Scaling relations are being measured that relate mixing rates, flame length, nitric oxide concentrations and flame blowout limits to recirculation strength. Efforts are being made to see if the scaling relations, based on a general recirculation strength, show any universality and might allow comparison of swirl-stabilized flames, central bluff-body flames, and dump-combustor flames, all of which utilize recirculation to enhance flame properties.

Evidence to date indicates that mixing with recirculation has some features that are fundamentally different from mixing in simple jets. For the swirl-stabilized flame studied, the internal recirculation causes the flame length to decrease by a factor of five from that of simple jet flames. Also, the flame length is no longer independent of fuel flowrate, as is the case of turbulent jet flames, for reasons that are discussed. Two physical mechanisms are observed from flow visualization that help explain the increase in mixing rates: (a) the coaxial fuel and air streams are abruptly brought to rest at the forward stagnation point of the recirculation zone, creating local vorticity due to the local opposing jet flows, and (b) large scale unsteady motion of the recirculation zone allows it to act like a large eddy which rapidly engulfs fluid into the upstream region of the recirculation zone. This latter concept differs from the previous concept that mixing takes place at the edge of (but not within) the recirculation zone.

A simple scaling concept is described, which is an extension of a well-known simple jet analysis but includes the effects of recirculation. Results to date show that a range of flame length data can be collapsed to a single curve. The scaling concepts explain three trends in the measurements.

Introduction

It is commonly known that enhanced mixing and improved flame stability can be achieved by creating internal recirculation within a flame. One can employ swirl, a central bluff body, or other sudden expansions in the flow such as in a dump-combustor[1-5]. The enhanced mixing usually results in shorter, more intense flames, but because of the larger temperatures and residence times, an increase in nitric oxide may result. However, because there are numerous conflicting theories, it cannot be said that the reasons why recirculation enhances mixing and flame stability are well known. For example, it is not clear if fuel-air mixing occurs deep within the recirculation zone, at the edge of the recirculation zone, or upstream of the recirculation zone. Some theories inherently assume that concentration fluctuations are only small perturbations to the mean concentration profiles, so that enhanced mixing can be explained by the fact that recirculation forces the local mean concentration gradients to increase. This small-scale diffusion concept is inherent to k-ε numerical models as well as to several flame blowout theories that utilize mean flow profiles[6-10] and local flame speeds.

More recent theories[11] and experiments show that mixing is due to an engulfment process, which instead is independent of the local mean concentration gradients. Related theories of flame blowout[12] have been proposed which also are based on engulfment. The fundamental question of how to model the mixing becomes even more important as the geometry and flowfield of the flame become more complicated than that of a simple jet. Rather than arguing about which theories give closer agreement with mean profiles, what are needed are flow visualization photographs and local measurements of "unmixedness" and mixing rates. The "ummixedness," as defined by Hawthorne et al.[13] and Libby and Williams[14] is large if the scalar fluctuations are appreciable. The overall mixing rate is simply inversely proportional to the flame length; it also can be measured by measuring the time required for flow on the flame centerline to be diluted to a stoichiometric concentration. A local mixing rate can be determined by measuring the gradient of the conserved scalar, since a rapid decrease of nozzle fluid on centerline implies rapid mixing.

The specific reasons why recirculation enhances mixing need to be quantified more carefully if general scaling laws are to be developed. A major problem is that recirculation is very geometry-dependent. The authors believe that a promising tactic is to separate the problem into two parts. There may be general scaling relations (which may be geometry independent) between flame properties and the recirculation strength, if properly defined. One possible definition of recirculation strength is given by the scaling concepts in the present paper. General scaling relations may allow for comparison of swirl, bluff-body and dump-combustor flames. The second part of the problem is the measurement of how recirculation strength depends on the specific geometry and flow conditions. An advantage of this tactic is that there is some evidence that the second part of the problem is not a strong function of the turbulent stresses, and may be modeled by using an inviscid model. For example, Batchelor[15] showed that for swirling flows, an inviscid model of the various forces (centrifugal, pressure, inertia) predicts that recirculation should occur and it predicts the location of the upstream stagnation point as well as the critical Swirl number. In the present research program, it was found that a numerical model correctly predicted the onset of recirculation and that the recirculation is governed primarily by radial pressure forces, centrifugal forces and geometry, and not by the turbulent stresses[16].

Another goal of the present program is to measure quantities that are useful in assessing computer models of recirculating flows, including vortex models (as they are being developed) and second-order models. However, rather than simply comparing mean profiles, it is felt that a more accurate test of models can be made by comparing when certain sudden and dramatic changes occur in a flowfield. Such changes occur in a swirling flame when: (a) there is the sudden onset of recirculation, (b) the central fuel jet first penetrates through the recirculation bubble, and (c) the flame blows out. It is important to quantify these limits in a systematic way and some measurements of these limits are discussed.

---

[*] Associate Professor, Member AIAA.
[**] Graduate Research Assistant.
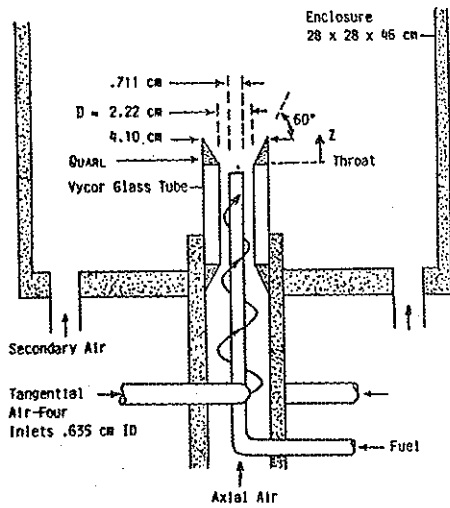[†] Currently Postdoctoral Fellow, UCSD, La Jolla CA.
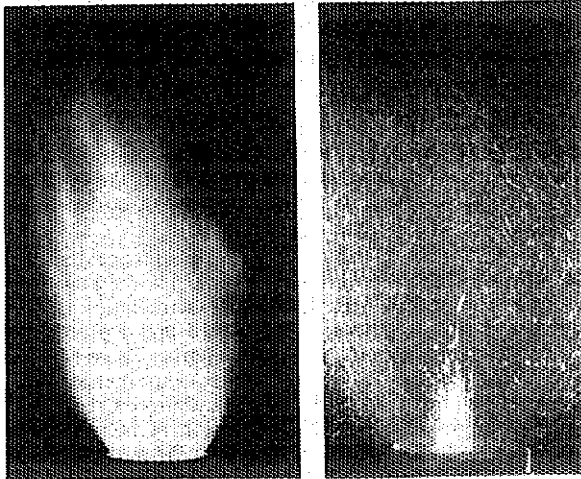
Figure 2. Photograph of swirl flame (S=1,
O_ϕ =0.67) and fuel flow visualization
using alumina particles in fuel only

Experiment

A swirl-stabilized flame which has strong internal recirculation was studied. The geometry of the apparatus is shown in Fig. 1. A more complete description is given in Ref. 3. The fuel was used either 100% methane or a mixture of 83% methane and 17% hydrogen by weight and was passed through a central fuel tube of diameter 0.711 cm. Swirling coaxial air passed through an outer tube of diameter 2.22 cm. Swirl number, representing the angular momentum/sec divided by the axial momentum per second (and normalized by the throat radius) varied from zero to four by varying the axial and tangential air flow rates. The Reynolds number was 20,000 and the air axial velocity at the throat was 12.7 m/sec. A metal or a Vycor glass diverging section, called a quarl, was used and is shown in Fig. 1.

Flow visualization was achieved by adding $TiCl_4$ to the fuel and later adding various amounts of water vapor to either the fuel or the air. Vater vapor results in the $TiCl_4$ forming TiO_2 particles which are visualized by a laser light sheet. The light sheet was formed by using a rotating mirror and focusing lens to sweep a 0.2 mm, 5-watt argon-ion laser beam across the field of view. To measure recirculation strength, the velocity fields in twelve flames were mapped out using LDV and the corresponding temperatures in the twelve flames were measured using Rayleigh scattering, as previously reported[3]. The characteristic recirculation velocity was determined by first determining the maximum width of the recirculation zone (i.e. the maximum distance between the centerline and the zero axial velocity contour, which is denoted b. At this axial location, the integral of $U2\pi rdr$ was then evaluated between centerline and the zero axial velocity contour, using the LDV. The recirculation velocity is defined as this integral divided by πb^2.

A photograph of the swirl-stabilized flame is shown in Fig. 2. The flow visualization in Fig. 2 shows that the fuel jet penetrates partially into the recirculation zone, but the fuel is turned backwards and then flows around the outside of the recirculation zone, which appears as the unseeded region in Fig. 2. The schematic shown in Fig. 3indicates that the zero axial velocity line must protrude upstream of the recirculating gases and the fuel and air may be mixed at that location. Methane flames were observed to be slightly lifted (by about 1 cm) but were stable; with 17% hydrogen added to the methane, the flames were attached to the fuel tube rim.

Velocity fields in three of the twelve flowfields that were mapped out are shown in Fig. 4; for comparison, the predicted flowfield using a TEACH axisymmetric, swirling flame numerical code is presented. The code was developed by Gosman and uses a PISO pressure-corrector algorithm to handle the important pressure gradients; it uses a Magnussen submodel to predict the local reaction rate. It was developed for bluff body combustors as well as for swirl flames. A detailed comparison of this model with the present flowfield measurements is described elsewhere[16]. The model did correctly predict the onset of recirculation, which is not sensitive to whatever turbulence submodel is used, at least in flows such as the present one in which the confining geometry and radial pressure gradients strongly influence recirculation. However, the model did not correctly predict the level of velocity fluctuations, scalar fluctuations (i.e. "unmixedness") or several other features of the mixing, which, of course, do depend strongly on the turbulence submodel. Vortex models may offer more promise and more direct comparison with flow visualization of the mixing process in the future.
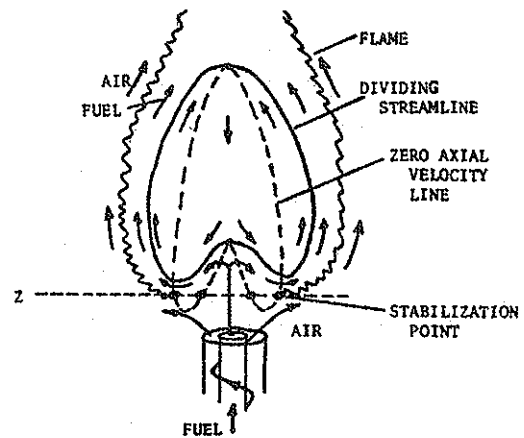

Figure 3. Schematic of the Forward
Stagnation Point Region

$\emptyset_0 = 0.0$
COLD FLOW

MEASURED   CALCULATED

$\emptyset_0 = 0.5$
FLAME

MEASURED   CALCULATED

$\emptyset_0 = 0.67$
FLAME

MEASURED   CALCULATED
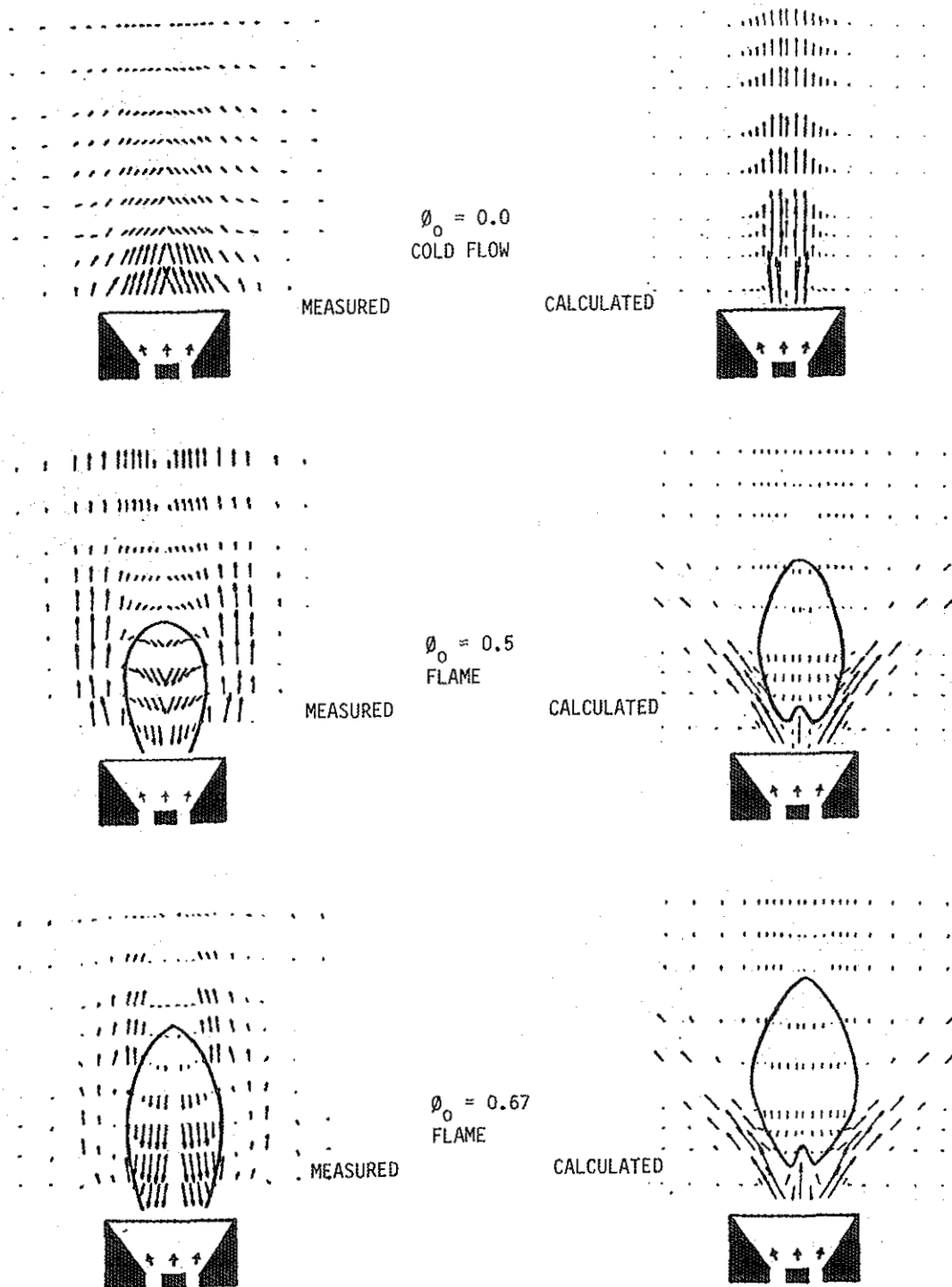
Figure 4.   Comparison of Measured and Calculated Velocity
             Fields Within Swirl-Stabilized Flames. Swirl
             Number = 1.0, overall fuel-air equivalence ratio
             $\emptyset_0$ as shown. Solid line is zero axial velocity
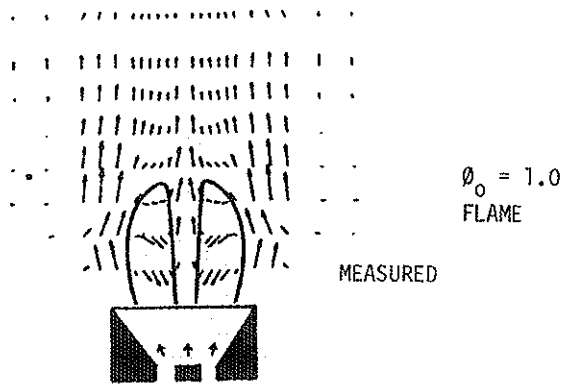   contour. Fuel = 83% CH_4, 17% H_2 by weight.

$\emptyset_0 = 1.0$
FLAME

MEASURED

Figure 4 (continued). Measured Velocity Field in Flame for S = 1.0, Showing Fuel Jet Penetration and Weakening of Recirculation Zone

No Recirculation
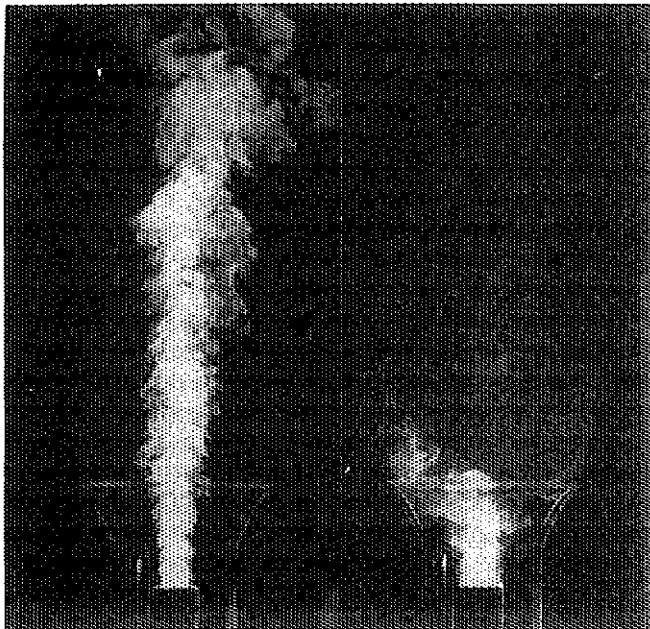S = 0.0

With Recirculation
S = 2.0

Figure 5. Enhanced Mixing Due To Recirculation. Same fuel flow rate and seeding in both cases. Light intensity indicates the conserved scalar: white = fuel, black = air, grey = mixed fluid.

Figure 4 shows two sudden changes that were measured: as heat release increases, there is a sudden onset of recirculation; and as the fuel jet velocity increases, the fuel jet suddenly penetrates through the recirculation zone, which decreases the recirculation strength and leads to blowout.

Results

Mixing is greatly enhanced by recirculation, as shown by Fig. 5. The fuel flowrate is held constant and is seeded with TiO_2 particles. The white region shown in Fig. 5 represents pure fuel, the black represents pure air, and the grey represents mixed fluid. It is seen that the overall mixing rate is enhanced
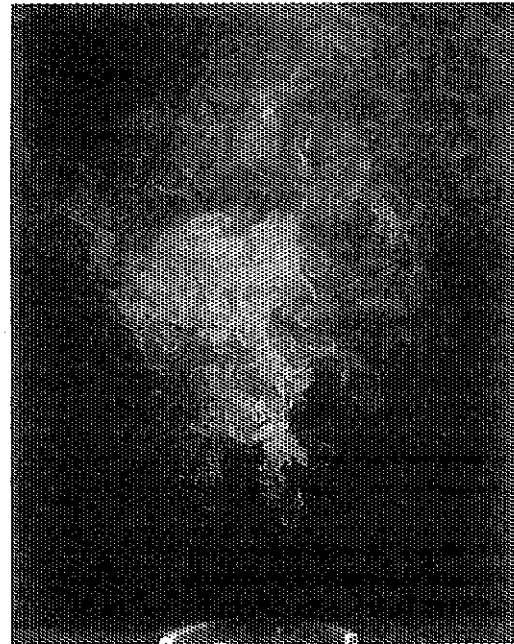

Figure 6. Visualization of Fuel That Has Mixed With Entrained Air. White = mixed fluid, black = pure fuel or air.

by recirculation because the distance required to mix the fuel with air is five times less than that required with no recirculation. The local mixing rate is being quantified by measuring the rate of decrease in the conserved scalar using single-point measurements.

The "unmixedness" at a point is related to the local concentration fluctuations[14]; equivalently, one may observe unmixedness if flow visualization indicates the presence of distinct regions of unmixed or partially mixed fluid. In Fig. 6, the mixing of the fuel and the entrained air is shown. $TiCl_4$ vapor is added to the fuel and the entrained air contains H_2O vapor. The white region in Fig. 6 is the mixed fluid while the black represents unmixed fuel or unmixed air. Unlike Fig. 5, which shows a rapid mixing between fuel and primary air, Fig. 6 shows that entrained air does not completely mix with the fuel as large regions of unmixedness occur. The reduced mixing in Fig. 6 also is due to the lack of a confining quarl geometry which reduces the recirculation strength.

The upstream boundary of the recirculation zone is visualized in Fig. 7; it is observed to move about in time and engulf large regions of fuel and air. The edge is unsteady and very irregular; these observations conflict with the concept that the recirculation zone is a steady fixed obstacle filled with products only, around which the fuel and air flow. The TiO_2 seed particles are observed to move in the negative z direction on axis but eventually move downstream and thus make it difficult to visualize the downstream boundary of the recirculation zone. Another problem is the fact that particles constantly move in the tangential direciton, thus are passing through the laser light sheet. Figure 8 shows the large degree of unmixedness in a simple jet. The fuel contains $TiCl_4$, the surrounding stagnant air contains H_2O, and the white regions represent mixed fluid while black represents unmixed fluid. While recirculating flows are not perfectly mixed, they clearly display more mixedness than the simple jet of Fig. 8; the degree of improved mixedness is being quantified in the present study.
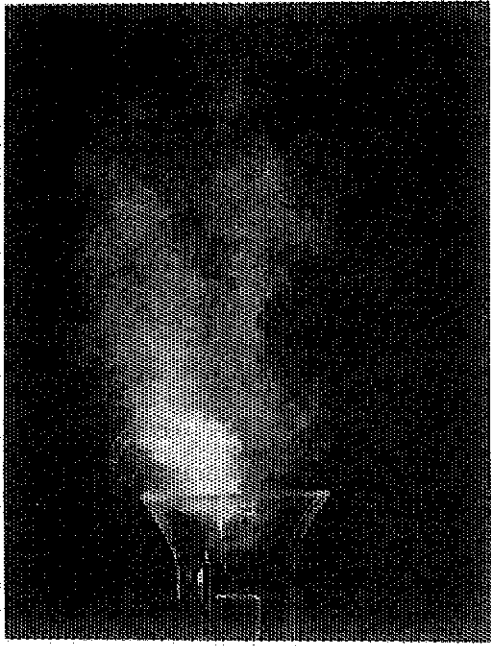
Figure 7. Visualization of the Recirculation Zone and Fluid that Has Left the Recirculation Zone.
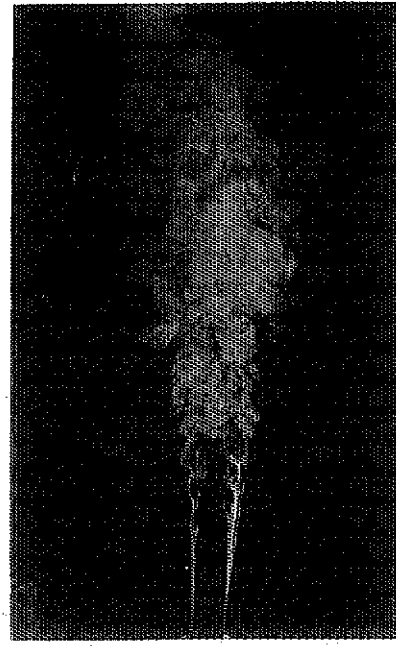

Figure 8. Visualization of Mixed Fluid in a Simple Non-Recirculating Jet. White = Mixed Fluid, Black = Pure Air or Pure Fuel
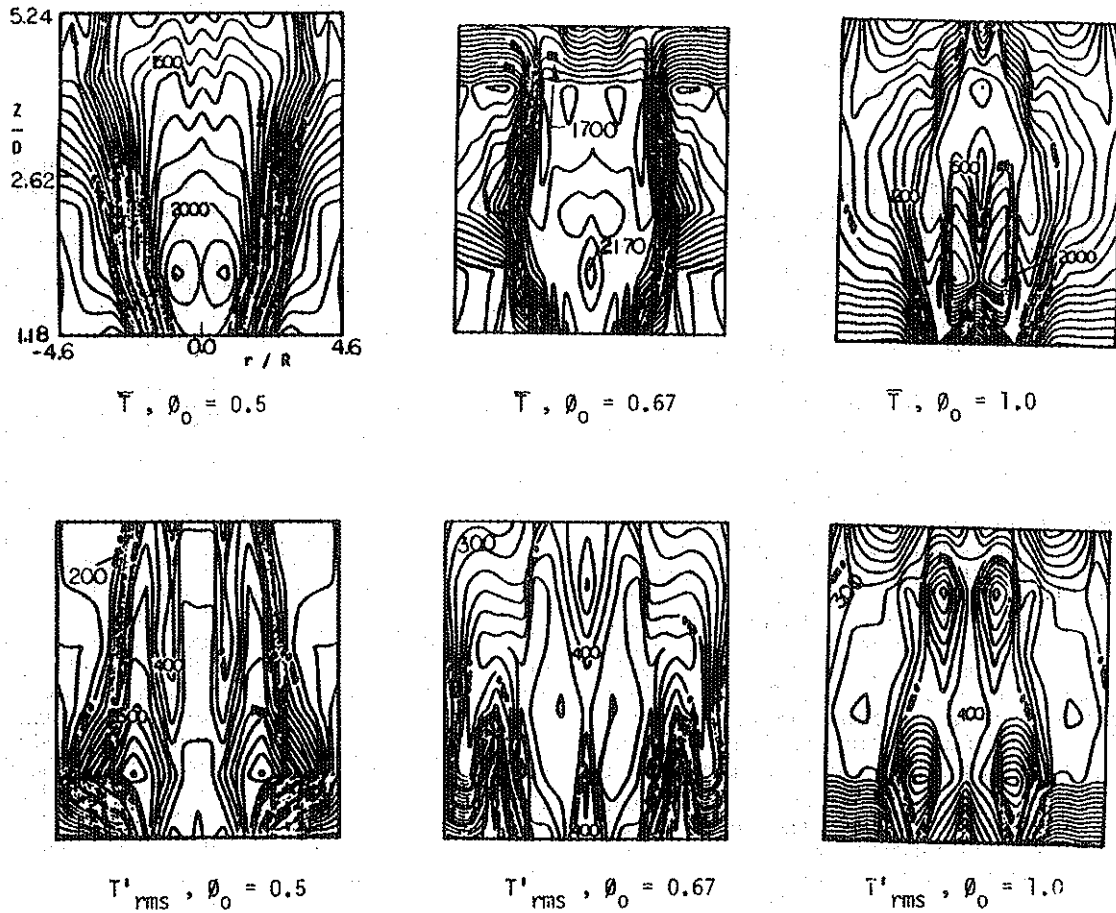

$\overline{T}$, ϕ_0 = 0.5

$\overline{T}$, ϕ_0 = 0.67

$\overline{T}$, ϕ_0 = 1.0

T'_{rms} , ϕ_0 = 0.5

T'_{rms} , ϕ_0 = 0.67

T'_{rms} , ϕ_0 = 1.0

Figure 9. Measured Mean and Fluctuating Temperatures in Degrees Kelvin Using Rayleigh Scattering; S = 1.

Normalized Flame Length L/d_f

Simple Jet Diffusion Flame
In Stagnant Air

100

80

60

40

20

$\phi_o = 1.0$

$\phi_o = 0.71$

$\phi_o = 0.50$

$\phi_o = 0.33$

$\phi_o = 0.25$

Actual Swirl Number S

1.0   2.0   3.0
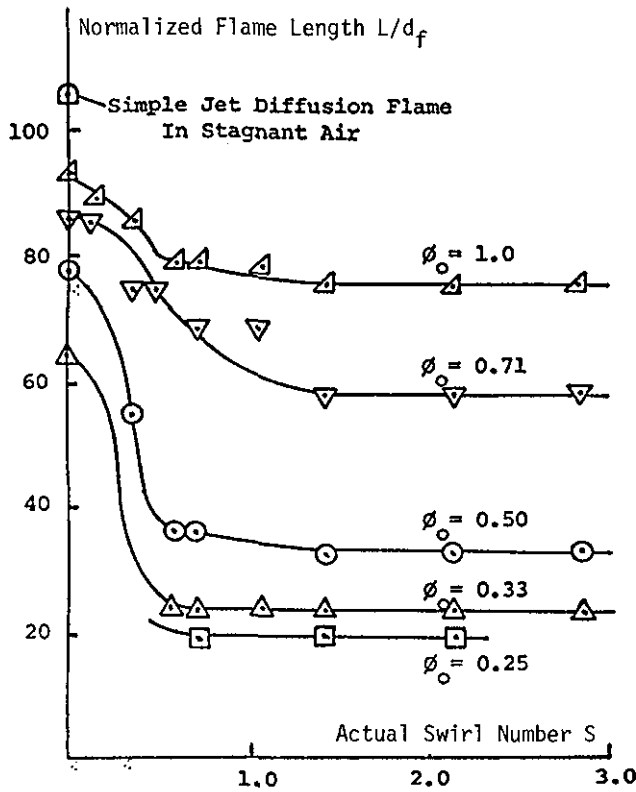
Figure 10. Measured Flame Length Showing Effects
of Swirl and Overall Fuel-Air Ratio ϕ_o

$\frac{U_{RZ}}{U_A}$

0.4

0.3

0.2

0.1

$\phi_o = .50$

Flame

$\phi_o = .67$

$\phi_o = 1.0$

Cold Flow $\phi = 0.0$

1.0   2.0

Actual Swirl Number

Figure 11. Measured Characteristic Recirculation
Zone Velocity U_{RZ} from LDV Data; Quarl
Angle = 60 degrees.

One measure of the "unmixedness" is the level of scalar fluctuations at a point, as pointed out by Hottel[13] and Libby and Williams[14]. Either the r.m.s. fluctuations in the conserved scalar, or the temperature fluctuations (T'_{rms}/T) are indicators of unmixedness since, in the limit of fast chemistry, temperature is a linear function of the conserved scalar. Typical values of T'_{rms}/T are 400K/2000K or 0.2 for the entire recirculation zone in the hydrogen-enriched flames in the present study, as shown by the Rayleigh scattering data in Fig. 9. This high level of unmixedness is expected near the edge of a jet but is surprising for locations within a recirculation zone, which has been assumed in numerous past studies to be "well-mixed" and approximated by a "perfectly stirred reactor."

The overall fuel-air mixing rate, on the other hand, can be quantified by simply measuring the flame lengths. Figure 10 shows how flame length decreases by a factor of five from that of a simple jet flame as the recirculation and the coaxial air flowrate are increased. This is consistent with the increased mixing shown in Fig. 5. Thus more rapid mixing results in shorter flames. In all cases in Fig. 10, the fuel flowrate is fixed. The three trends observed in Fig. 10 are: (a) flames become shorter as recirculation increases; (b) flames become shorter as the amount of coaxial air flow rate increases (i.e. as ϕ_o, the overall fuel-air equivalence ratio, decreases); (c) for swirl numbers above 1.0 there is little change in flame height, implying that increased swirl no longer increases recirculation.

To relate recirculation strength to swirl, the recirculation zone was measured using the method described previously; the characteristic velocity U_{RZ} is shown in Fig. 11. As implied by observation (c) above, recirculation strength does not increase for swirl numbers exceeding about 1.0 to 1.5 for the present geometry. The physical reasons are as follows. As the swirl
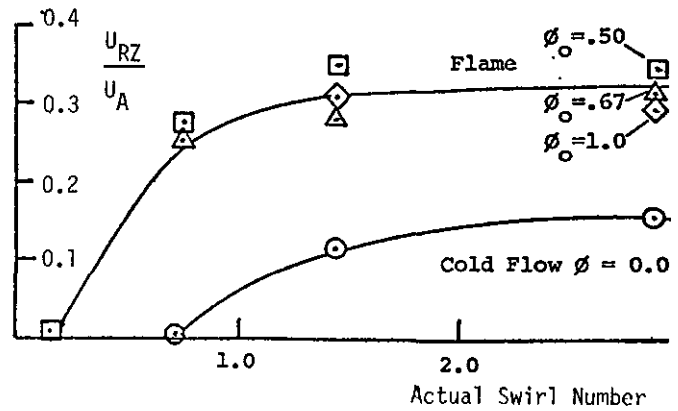
number increases, the pressure on centerline will decrease and the velocity of gas that recirculates increases; however U_A is held constant and it is unreasonable to expect that the recirculating velocity U_{RZ} will continue to increase without limit; i.e. it is unreasonable to expect that the gas inside the recirculation zone could ever have a velocity that exceeds the velocity of gas that passes around the outside of the recirculation zone. Therefore the curve shown in Fig. 11 asymptotes to some maximum value of U_{RZ}/U_A.

Scaling Concepts

A better understanding of why the flame length is decreased by recirculation, as was shown in Fig. 10, can be gained from a simple "thought experiment." One can combine the ideas of Hottel's[13] classic predictions of flame lengths of jet flames with some well-known entrainment rates of simple shear layers. However, the concepts that follow are not a rigorous scaling analysis of the governing equations nor do they constitute a model. However, they do provide a useful guide to the experiments.

We first consider a simple shear layer as shown in Fig. 12b and ask, "What is the volume per second of fuel and air that is entrained into a shear layer?" This problem has been exhaustively studied by Brown and Roshko[17], Dimotakis and Brown[18] and Briedenthal[19]. The volume/sec entrained is the flow that crossed the shear layer boundaries, and is proportional to $d\delta/dz$ where δ is the layer width. Since $d\delta/dz$ is proportional to ΔU (the difference between fuel and air velocities), the volume/sec entrained by a segment of the shear layer that has a distance L in the z direction is proportional to ΔU $L(2\pi b)$ where $2\pi b$ is the circumference of the axisymmetric shear layer as shown in Fig. 12. Briedenthal[19] has shown that the volume/sec of fluid that is mixed uniformly at the molecular level is proportional to that which is entrained.

We now ask, "How is a flame length affected if the air entrainment rate is increased by somehow increasing the local vortex strength?" Hottel[13] showed that flame length L is determined by the criterion that the volumetric flowrate of fuel $(U_F \pi d_F^2)$ divided by the total volume/sec of air entrained must equal the stoichiometric molar fuel-air ratio (C_S). Hottel assumed that small scale mixing occurred so that his criterion for flame length is:

$$c_S = \frac{\text{volume/sec fuel}}{\text{volume/sec air entrained}} = \frac{\pi \, d_F^2 U_F \text{ constant}}{D(\partial c/\partial r)(\pi \, d_F \, L)} = \frac{\pi d_F^2 U_F \text{ const.}}{u'b(1/d_F)d_F \, L} \quad (1)$$

where the volume/sec/area of air entrained is assumed to be $D \, \partial c/\partial r$, which is a gradient diffusion concept. The diffusivity D is assumed by Hottel to scale as $u'b$ where u' is the characteristic r.m.s. velocity fluctuation and b is a characteristic mixing distance.

Rather than use the small-scale mixing argument of Hottel, one can use the volume/sec of air entrained into a free shear layer that is given above, and one obtains exactly the same scaling result that is predicted by equation (1) except that u' in equation (1) is replaced by ΔU so that flame length L becomes:

$$L = \frac{U_F \, d_F^2 \cdot \text{constant}}{(\Delta U \, b) \, c_S} \quad (2)$$
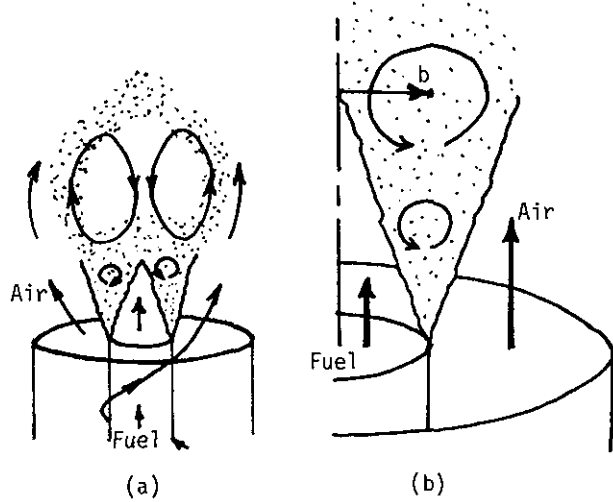

Figure 12. Schematic of Flame Having Internal Recirculation (a) and the Simpler Case of Mixing in a Shear Layer (b).

Equation (2) thus is a scaling which is based on well-known shear layer concepts and not on small scale mixing, but because u' is proportional to ΔU, the scaling argument is identical to that of Hottel. It is now noted that the quantity $\Delta U b$ in the denominator of equation (2) represents a vortex strength, or circulation. The rotational velocity of a vortex structure in a shear layer is characterized by the velocity at its outer edge, with respect to the velocity at its center. This rotational velocity is $U_1 - (U_1 + U_2)/2$ or simply $\Delta U/2$.

Therefore, if the vortex strength $\Delta U b$ is increased, equation (2) shows that air entrainment rates increase and flame lengths decrease. For the central recirculation zone shown in Fig. 11a, we can define an "effective vortex strength," which is a circulation, as:

$$\Delta U b \equiv c_1 U_{RZ} b + c_2 |U_F - U_A| d_F \quad (3)$$

where U_{RZ} is some velocity that is characteristic of the increased vorticity that is to be produced by recirculation and c_1 and c_2 are constants. The quantity $|U_F - U_A| d_F$ represents the

vortex strength associated with the simple shear flow that occurs when U_{RZ} is zero; it is identical to the scaling used by Hottel. For comparison with experiment, it is convenient to define the overall fuel-air equivalence ratio ϕ_0 as $(U_F \, d_F^2/U_A \, d_A^2)/c_S$ where U_A and d_A are the axial velocity and diameter of the air flow at the burner exit.

The resulting flame length (L) of this hypothetical thought experiment is obtained by combining equations (2-3) and the above definition of ϕ_0 to yield:

$$\frac{L}{d_F} = \frac{(\text{constant}) \, \phi_0 \, (d_A/d_F)}{\left(\dfrac{U_{RZ}}{U_A} \dfrac{b}{d_A} + (\text{constant}) \, \dfrac{|U_A - U_F|}{U_A} \right)} \quad (4)$$

Equation (4) does explain four trends that have been measured: (a) For a simple jet flame with no recirculation and no coaxial air, U_{RZ} and U_A are zero and equation (4) becomes $L/d = \text{constant}/c_S$, which is exactly the well-known result of Hottel, as expected. (b) Coaxial jet flames with no recirculation ($U_{RZ} = 0$) are predicted to become shorter as coaxial air U_A increases; this is verified by the measurements in Fig. 10. (c) The flame length for a fixed recirculation velocity (U_{RZ}) should increase as the fuel flowrate, and thus ϕ_0 increases; this trend was previously measured by the present authors[3] and this trend also is seen in the data of Fig. 10.

Therefore, the present flame with recirculation is different from a simple jet flame in the following way. Mixing in a simple jet flame increases as fuel flowrate increases; thus the flame length, as given by equation (2), remains constant. Mixing with recirculation is controlled by the air flow primarily, so that if air flow is fixed and fuel flowrate increases, the flame becomes longer, similar to a laminar diffusion flame. (d) Most importantly, equation (4) shows that flame height decreases as recirculation velocity increases.

Comparison of Various Swirl and Bluff-Body Flames

A useful concept arising from equation (4) is that perhaps flame length measurements obtained over a range of conditions or geometries might be correlated if the recirculation strength is properly defined and measured. While a more rigorous scaling analysis presently is in progress, some preliminary results appear to be encouraging when the circulation strength $U_{RZ} \cdot b$, as suggested by equation (4), is used. U_{RZ} was measured using laser velocimetry as was shown in Fig. 11. A measure of the width of the recirculation vortex b is the measured maximum radius of the zero axial velocity contour. The preliminary results shown in Fig. 13 show that by normalizing flame height as suggested by equation (4) and by using $U_{RZ} \cdot b$ as the independent parameter, the flame height data collapse to a single curve. Future work is planned to improve the scaling concepts, to systematically vary the parameters in equation (4), and to plot bluff body flame lengths on a curve similar to Fig. 12 so as to assess the similarities between swirl and bluff body flames.

The Onset of Recirculation and Flame Blowout

It is useful to quantify two conditions for which sudden and dramatic changes in the flowfield occur, namely the onset of recirculation and flame blowout. For future flame models (whether they be vortex models, entrainment models, or second order models) to be considered successful, they must be able to explain and perhaps predict the measured sudden changes in the flame. The critical swirl number that causes the flow to begin to recirculate is shown in Fig. 14. Recirculation

is detected by inserting TiO_2 particles in the cold flows and by inserting a wire covered with saltwater into the flames. The NaCl or TiO_2 is first inserted far downstream and the insertion location is moved upstream until the NaCl or TiO_2 tracer is observed to move in the negative z direction on centerline, which indicates the presence of recirculation. Figure 14 shows that both heat release and the quarl significantly enhance the onset of recirculation. However, larger fuel jet velocities (which occur as ϕ_0 is increased in Fig. 14) are observed to cause a suppression of the onset of recirculation, since the fuel jet can penetrate through and weaken the recirculation region, as was shown in Fig. 4c.

The flame blowout limits are shown in Figs. 15 and 16. For each graph, the total air flow was held fixed and the swirl number and fuel flow was varied. The three-sided stable region of Fig. 15a demonstrates that there are three distinct blowout limits. The limits correspond to the (a) maximum swirl limit associated with flame strain out, (b) maximum fuel flow rate (i.e., minimum value of $1/\phi_0$ on Fig. 15) due to the fuel jet penetrating and weakening the recirculation zone, and (c) minimum swirl limit associated with the onset of recirculation. Flow visualization experiments are in progress to better understand the three measured blowout limits. Currently, three criteria for flame blowout have been proposed: (a) the local normal gas velocity everywhere exceeds the local turbulent flame speed[7,9,10,20], (b) too many holes are created in the flame sheet due to local flame strain-out[21], and (c) excessive amounts of cold air are mixed too rapidly with the hot products[12]. Additional research is needed before any of the above criteria can be discounted or verified.

References

1. Beer, J.M. and Chigier, N.A. Combustion Aerodynamics, Wiley, New York, 1972.

2. Gupta, A.K., Beer, J.M. and Swithenbank, J., 16th Symp. on Combustion, 1977.

3. Tangirala, V., Chen, R.H. and Driscoll, J.F., Comb. Sci. Tech. 51, 75, 1986.

4. Halthorne, A.N. and Gouldin, F.C., AIAA J. 24, 1129, 1986.

5. LaRue, J.C., Samuelson, G.S. and Seiler, E.T., 20th Symp. on Combustion, 1985.

6. Lenze, B., 19th Symp. on Comb., 565, 1982.

7. Chakravarty, A., Lockwood, F.C. and Sinicropi, G., Comb. Sci. Tech. 42, 67, 1984.

8. Leschziner, M.A. and Rodi, W., AIAA J. 22, 1742, 1984.

9. Leuckel, W. and Fricker, N., J. Inst. Fuel 49, 152, 1976.

10. Yuasa, S., Comb. Flame 66, 181, 1986.

11. Broadwell, J.E. and Dimotakis, P.E., AIAA J. 24, 6, 1986.

12. Broadwell, J.E., Dahm, W.J.A. and Mungal, G., 20th Symp. on Combustion, 1985.

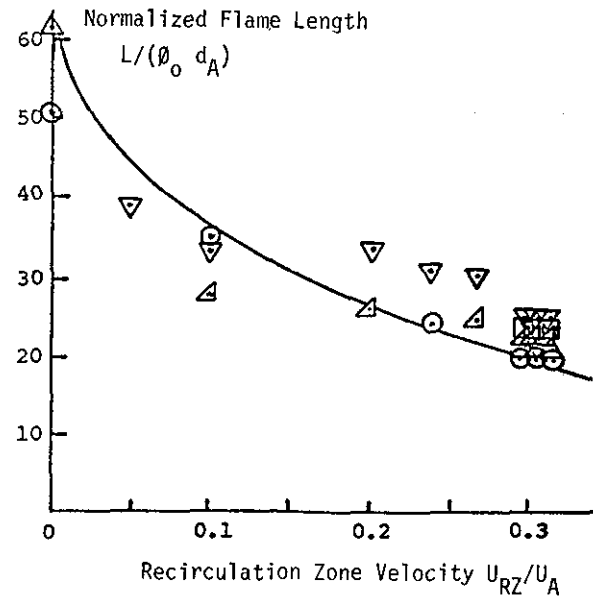13. Hawthorne, W.R., Weddell, D.S. and Hottel, H.C., 3rd Symp. on Combustion, 1943.

Figure 13. Flame Length Data of Figure 10 Collapsed to a Single Curve by Using U_{RZ} and by Normalizing L as Suggested by Equation 4.
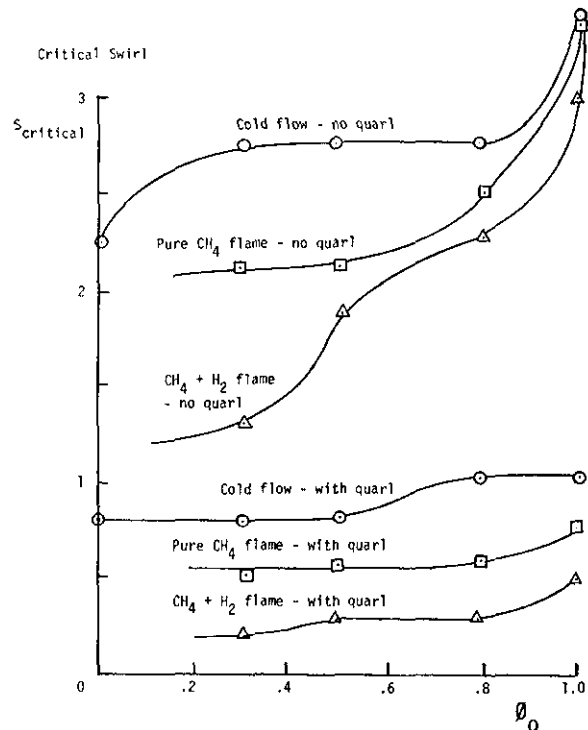

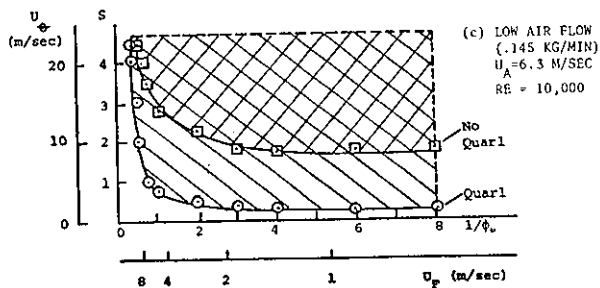Figure 14. Critical Swirl Number That Causes the Onset of Recirculation.

Figure 15. Flame Blowout Limits for a Swirl-Stabilized Methane Flame. Shaded Region is Stable. U_A, U_θ = Axial, Tangential Throat Air Velocity, U_F = Fuel Exit Velocity
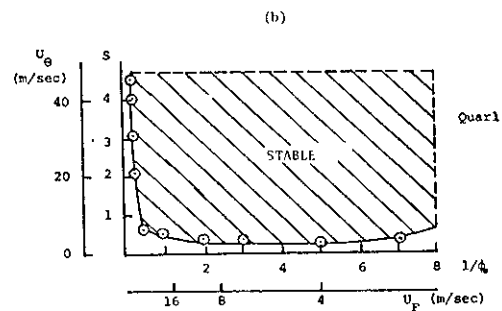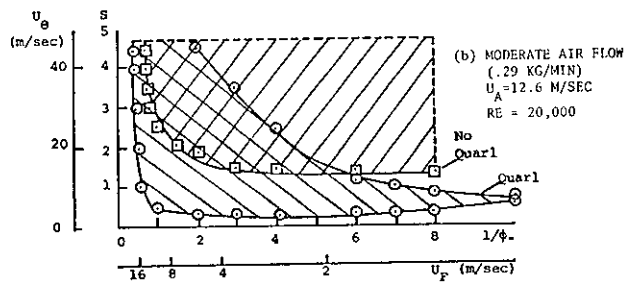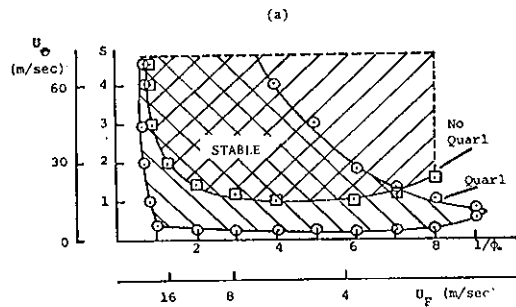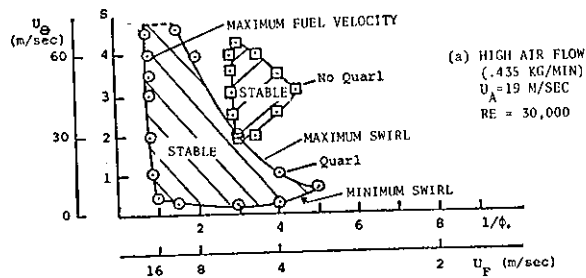

Figure 16. Flame Blowout Limits for Hydrogen-Enriched Methane Flames; (a) 8% H_2 by weight, (b) 17% H_2

14. Libby, P.A. and Williams, F.A., Turbulent Reacting Flow, Springer-Verlag, Berlin.

15. Batchelor, G.K., Intro. to Fluid Mechanics, Cambridge, University Press.

16. Tangirala, V., Paper 6A2 Central States Meeting of the Combustion Institute, Cleveland, 1986.

17. Brown, G. L. and Roshko, A., J. Fluid Mech. 64, 775, 1974.

18. Dimotakis, P. E. and Brown, G. L., J. Fluid Mech. 78, 535, 1976.

19. Breidenthal, R., J. Fluid Mech. 109, p. 1, 1981.

20. Vanquickenborne, L. and VanTiggelen, A., Comb. Flame 10, 59, 1966.

21. Peters, N. and Williams, F.A., AIAA J. 21, 423, 1983.